On simulations of SPDE-based stationary Random Fields

R. Carrizo Vergara, N. Desassis , D. Allard

MINES ParisTech

Workshop INLA-SPDE

Avignon, France

8th November 2018

Section 1

Introduction

Simulations within the SPDE Approach

In the SPDE Approach [Lindgren et al., 2011] we relate the studied Random Field to a SPDE: we avoid to work explicitly with covariance functions and matrices.

Simulations within the SPDE Approach

In the SPDE Approach [Lindgren et al., 2011] we relate the studied Random Field to a SPDE: we avoid to work explicitly with covariance functions and matrices.

Simulations can be performed solving the SPDE through a PDE numerical method:

Simulations within the SPDE Approach

In the SPDE Approach [Lindgren et al., 2011] we relate the studied Random Field to a SPDE: we avoid to work explicitly with covariance functions and matrices.

Simulations can be performed solving the SPDE through a PDE numerical method:

- Finite Difference Method.

Simulations within the SPDE Approach

In the SPDE Approach [Lindgren et al., 2011] we relate the studied Random Field to a SPDE: we avoid to work explicitly with covariance functions and matrices.

Simulations can be performed solving the SPDE through a PDE numerical method:

- Finite Difference Method.
- Finite Element Method.

Simulations within the SPDE Approach

In the SPDE Approach [Lindgren et al., 2011] we relate the studied Random Field to a SPDE: we avoid to work explicitly with covariance functions and matrices.

Simulations can be performed solving the SPDE through a PDE numerical method:

- Finite Difference Method.
- Finite Element Method.
- Spectral Method (in the PDE sense).

Simulations within the SPDE Approach

In the SPDE Approach [Lindgren et al., 2011] we relate the studied Random Field to a SPDE: we avoid to work explicitly with covariance functions and matrices.

Simulations can be performed solving the SPDE through a PDE numerical method:

- Finite Difference Method.
- Finite Element Method.
- Spectral Method (in the PDE sense).

Issue:

These methods are often conceived under the context of a particular operator. They cannot simply be applied under more general SPDEs without suitable adaptations.

A *spectral method*

In this presentation we study an already existent method for simulating stationary random fields.

- [Pardo-Iguzquiza and Chica-Olmo, 1993]: conception in a geostatistical context with applications.
- [Lang & Potthoff, 2011]: conception in a SPDE context.

A *spectral method*

In this presentation we study an already existent method for simulating stationary random fields.

- [Pardo-Iguzquiza and Chica-Olmo, 1993]: conception in a geostatistical context with applications.
- [Lang & Potthoff, 2011]: conception in a SPDE context.

Advantages

This method is *quite general*, and it will allow us to obtain simulations for models beyond the Matérn model and being related to SPDEs involving a wide-class of pseudo-differential operators.

A *spectral method*

In this presentation we study an already existent method for simulating stationary random fields.

- [Pardo-Iguzquiza and Chica-Olmo, 1993]: conception in a geostatistical context with applications.
- [Lang & Potthoff, 2011]: conception in a SPDE context.

Advantages

This method is *quite general*, and it will allow us to obtain simulations for models beyond the Matérn model and being related to SPDEs involving a wide-class of pseudo-differential operators.

This method can be catalogued as a *spectral method* in both PDE and geostatistical senses.

Section 2

Theoretical Principles

Principles

We consider a *Riemann sequence of partitions growing to* $\mathbb{R}^d$:
$(V_j^N)_{j\in\{1,\ldots,N\},N\in\mathbb{N}_*}$, a collection of bounded Borel sets of $\mathbb{R}^d$ such that

Principles

We consider a *Riemann sequence of partitions growing to* $\mathbb{R}^d$:
$(V_j^N)_{j\in\{1,\dots,N\},N\in\mathbb{N}_*}$, a collection of bounded Borel sets of $\mathbb{R}^d$ such that

- $V_j^N \cap V_k^N = \emptyset$, for all $j, k \in \{1, ..., N\}$ such that $j \neq k$, for all $N \in \mathbb{N}_*$

Principles

We consider a *Riemann sequence of partitions growing to* $\mathbb{R}^d$:
$(V_j^N)_{j\in\{1,\dots,N\},N\in\mathbb{N}_*}$, a collection of bounded Borel sets of $\mathbb{R}^d$ such that

- $V_j^N \cap V_k^N = \emptyset$, for all $j, k \in \{1, ..., N\}$ such that $j \neq k$, for all $N \in \mathbb{N}_*$
- $\ell_N := \max_{j\in\{1,\dots,N\}} \text{diam}(V_j^N) \to 0$ as $N \to \infty$

Principles

We consider a *Riemann sequence of partitions growing to* $\mathbb{R}^d$:
$(V_j^N)_{j\in\{1,\dots,N\},N\in\mathbb{N}_*}$, a collection of bounded Borel sets of $\mathbb{R}^d$ such that

- $V_j^N \cap V_k^N = \emptyset$, for all $j, k \in \{1, ..., N\}$ such that $j \neq k$, for all $N \in \mathbb{N}_*$
- $\ell_N := \max_{j\in\{1,\dots,N\}} \operatorname{diam}(V_j^N) \to 0$ as $N \to \infty$
- for all $K \subset \mathbb{R}^d$ compact, there exists $N_0 \in \mathbb{N}$ such that for all $N \geq N_0$, $K \subset \bigcup_{j=1}^N V_j^N$

Principles

We consider a *Riemann sequence of partitions growing to* $\mathbb{R}^d$:
$(V_j^N)_{j\in\{1,\dots,N\},N\in\mathbb{N}_*}$, a collection of bounded Borel sets of $\mathbb{R}^d$ such that

- $V_j^N \cap V_k^N = \emptyset$, for all $j, k \in \{1, ..., N\}$ such that $j \neq k$, for all $N \in \mathbb{N}_*$
- $\ell_N := \max_{j\in\{1,\dots,N\}} \operatorname{diam}(V_j^N) \to 0$ as $N \to \infty$
- for all $K \subset \mathbb{R}^d$ compact, there exists $N_0 \in \mathbb{N}$ such that for all $N \geq N_0$, $K \subset \bigcup_{j=1}^N V_j^N$

We consider in addition a collection of *tag-points*: $(\xi_j^N)_{j\in\{1,\dots,N\},N\in\mathbb{N}_*} \subset \mathbb{R}^d$, such that $\xi_j^N \in V_j^N$, for all $j \in \{1, ..., N\}, N \in \mathbb{N}_*$.

Principles

We consider a *Riemann sequence of partitions growing to* $\mathbb{R}^d$:
$(V_j^N)_{j\in\{1,\dots,N\},N\in\mathbb{N}_*}$, a collection of bounded Borel sets of $\mathbb{R}^d$ such that

- $V_j^N \cap V_k^N = \emptyset$, for all $j,k \in \{1,...,N\}$ such that $j \neq k$, for all $N \in \mathbb{N}_*$
- $\ell_N := \max_{j\in\{1,\dots,N\}} \text{diam}(V_j^N) \to 0$ as $N \to \infty$
- for all $K \subset \mathbb{R}^d$ compact, there exists $N_0 \in \mathbb{N}$ such that for all $N \geq N_0$, $K \subset \bigcup_{j=1}^N V_j^N$

We consider in addition a collection of *tag-points*: $(\xi_j^N)_{j\in\{1,\dots,N\},N\in\mathbb{N}_*} \subset \mathbb{R}^d$, such that $\xi_j^N \in V_j^N$, for all $j \in \{1,...,N\}, N \in \mathbb{N}_*$.

Inspiration

If μ is a locally finite measure over $\mathbb{R}^d$, it can be approximated by

$$\mu_N = \sum_{j=1}^N \mu(V_j^N)\delta_{\xi_j^N} \quad (1)$$

Principles

If Z is a real stationary Random Field over $\mathbb{R}^d$, then $M_Z = \mathscr{F}(Z)$ is an Hermitian slow-growing orthogonal Random Measure.

PRINCIPLES

If Z is a real stationary Random Field over $\mathbb{R}^d$, then $M_Z = \mathscr{F}(Z)$ is an Hermitian slow-growing orthogonal Random Measure.

APPROXIMATING THE ORTHOGONAL RANDOM MEASURE

$$M_{Z_N} := \sum_{j=1}^{N} M_Z(V_j^N)\delta_{\xi_j^N} \quad (2)$$

Principles

If Z is a real stationary Random Field over $\mathbb{R}^d$, then $M_Z = \mathscr{F}(Z)$ is an Hermitian slow-growing orthogonal Random Measure.

Approximating the orthogonal Random Measure

$$M_{Z_N} := \sum_{j=1}^{N} M_Z(V_j^N)\delta_{\xi_j^N} \tag{2}$$

Approximating the field

$$Z_N(x) := \mathscr{F}^{-1}\left(\sum_{j=1}^{N} M_Z(V_j^N)\delta_{\xi_j^N}\right)(x) = \frac{1}{(2\pi)^{\frac{d}{2}}}\sum_{j=1}^{N} M_Z(V_j^N)e^{ix^T\xi_j^N} \tag{3}$$

Principles

If Z is a real stationary Random Field over $\mathbb{R}^d$, then $M_Z = \mathscr{F}(Z)$ is an Hermitian slow-growing orthogonal Random Measure.

Approximating the orthogonal Random Measure

$$M_{Z_N} := \sum_{j=1}^{N} M_Z(V_j^N)\delta_{\xi_j^N} \tag{2}$$

Approximating the field

$$Z_N(x) := \mathscr{F}^{-1}\left(\sum_{j=1}^{N} M_Z(V_j^N)\delta_{\xi_j^N}\right)(x) = \frac{1}{(2\pi)^{\frac{d}{2}}}\sum_{j=1}^{N} M_Z(V_j^N)e^{ix^T\xi_j^N} \tag{3}$$

The random variables $M_Z(V_j^N)$ are non-correlated complex random variables, with variance

$$\mathbb{V}ar(M_Z(V_j^N)) = (2\pi)^{\frac{d}{2}}\mu_Z(V_j^N), \tag{4}$$

where μ_Z is the spectral measure of Z.

Principles

$(Z_N(x))_{x\in\mathbb{R}^d}$ is a (complex) stationary Random Function with spectral measure and covariance

$$\mu_{Z_N} = \sum_{j=1}^{N} \mu_Z(V_j^N)\delta_{\xi_j^N} \quad ; \quad \rho_{Z_N}(h) = \frac{1}{(2\pi)^{\frac{d}{2}}} \sum_{j=1}^{N} \mu_Z(V_j^N) e^{ih^T \xi_j^N}. \tag{5}$$

Result

If Z is a real and (mean-square) continuous stationary Random Function over $\mathbb{R}^d$, then

$$\sup_{x\in K} \mathbb{E}\left(\left|Z(x) - Z_N(x)\right|^2\right) \to 0, \quad \text{as } N \to \infty, \forall K \subset \mathbb{R}^d \text{ compact.} \tag{6}$$

Principles

$(Z_N(x))_{x\in\mathbb{R}^d}$ is a (complex) stationary Random Function with spectral measure and covariance

$$\mu_{Z_N} = \sum_{j=1}^{N} \mu_Z(V_j^N)\delta_{\xi_j^N} \quad ; \quad \rho_{Z_N}(h) = \frac{1}{(2\pi)^{\frac{d}{2}}} \sum_{j=1}^{N} \mu_Z(V_j^N) e^{ih^T \xi_j^N}. \tag{5}$$

Result

If Z is a real and (mean-square) continuous stationary Random Function over $\mathbb{R}^d$, then

$$\sup_{x\in K} \mathbb{E}\left(|Z(x) - Z_N(x)|^2\right) \to 0, \quad \text{as } N \to \infty, \forall K \subset \mathbb{R}^d \text{ compact.} \tag{6}$$

Vanishing bound

$$\sup_{x\in K} \mathbb{E}\left(|Z(x) - Z_N(x)|^2\right) \leq \frac{1}{(2\pi)^{\frac{d}{2}}} \left[4\ell_N^2 \mu_Z(\mathbb{R}^d) \sup_{x\in K} |x|^2 + \mu_Z\left(\mathbb{R}^d \setminus \bigcup_{j=1}^{N} V_j^N\right)\right] \tag{7}$$

Remark: Generalized version

If Z is a real stationary Generalized Random Field over $\mathbb{R}^d$ (slow-growing spectral measure, not necessarily finite), then

$$\mathbb{E}\left(\left|\langle Z,\varphi\rangle - \langle Z_N,\varphi\rangle\right|^2\right) \to 0, \quad \text{as } N \to \infty, \forall \varphi \in \mathscr{S}(\mathbb{R}^d) \tag{8}$$

Application to SPDEs

Consider a SPDE over $\mathbb{R}^d$ of the form

$$\mathcal{L}_g U = X, \tag{9}$$

where X is a real stationary Random Field over $\mathbb{R}^d$ and $\mathcal{L}_g = \mathscr{F}^{-1}(g\mathscr{F}(\cdot))$, with $g : \mathbb{R}^d \to \mathbb{C}$ an Hermitian ($\overline{g(\xi)} = g(-\xi)$) continuous polynomially bounded function (*symbol function*).

Application to SPDEs

Consider a SPDE over $\mathbb{R}^d$ of the form

$$\mathcal{L}_g U = X, \tag{9}$$

where X is a real stationary Random Field over $\mathbb{R}^d$ and $\mathcal{L}_g = \mathscr{F}^{-1}(g\mathscr{F}(\cdot))$, with $g : \mathbb{R}^d \to \mathbb{C}$ an Hermitian ($\overline{g(\xi)} = g(-\xi)$) continuous polynomially bounded function (*symbol function*).

Fact [Carrizo Vergara et al., 2018]

If g is inferiorly bounded by the inverse of a strictly positive polynomial, there exists a unique stationary solution given by

$$U = \mathcal{L}_{\frac{1}{g}} X \tag{10}$$

Application to SPDEs

Consider a SPDE over $\mathbb{R}^d$ of the form

$$\mathcal{L}_g U = X, \tag{9}$$

where X is a real stationary Random Field over $\mathbb{R}^d$ and $\mathcal{L}_g = \mathscr{F}^{-1}(g\mathscr{F}(\cdot))$, with $g : \mathbb{R}^d \to \mathbb{C}$ an Hermitian ($\overline{g(\xi)} = g(-\xi)$) continuous polynomially bounded function (*symbol function*).

Fact [Carrizo Vergara et al., 2018]

If g is inferiorly bounded by the inverse of a strictly positive polynomial, there exists a unique stationary solution given by

$$U = \mathcal{L}_{\frac{1}{g}} X \tag{10}$$

IDEA [Lang & Potthoff, 2011]

Replace X with its approximation X_N and then,

$$U_N(x) = \mathcal{L}_{\frac{1}{g}} X_N(x) = \mathscr{F}^{-1}\left(\frac{1}{g}\sum_{j=1}^{N} M_X(V_j^N)\delta_{\xi_j^N}\right)(x) = \frac{1}{(2\pi)^{\frac{d}{2}}}\sum_{j=1}^{N}\frac{M_X(V_j^N)}{g(\xi_j^N)}e^{ix^T\xi_j^N} \tag{11}$$

Application to SPDEs

Result (generalized version)

$$\mathbb{E}\left(\left|\langle U,\varphi\rangle - \langle U_N,\varphi\rangle\right|^2\right) \to 0, \quad \text{as } N\to\infty, \forall \varphi \in \mathscr{S}(\mathbb{R}^d) \tag{12}$$

(Not precise) Result

If $|g|^{-2}$ is integrable with respect to μ_X, U is a continuous stationary Random Function. Under suitable conditions on g and/or X,

$$\sup_{x\in K} \mathbb{E}\left(\left|U(x) - U_N(x)\right|^2\right) \to 0, \quad \text{as } N\to\infty, \forall K \subset \mathbb{R}^d \text{ compact.} \tag{13}$$

Section 3

Implementation and Illustrations

Implementation Details

Implementation Details

- The Random Function U_N is periodic $\rightarrow$ restrict the evaluation to a domain.

Implementation Details

- The Random Function U_N is periodic $\rightarrow$ restrict the evaluation to a domain.
- The Random Function U_N is complex. If a real approximation is desired, the sequence of partitions $(V_j^N)_{j\in\{1,\dots,N\},N\in\mathbb{N}_*}$ and the tag points $(\xi_j^N)_{j\in\{1,\dots,N\},N\in\mathbb{N}_*}$ must be selected such that $M_{U_N} = \mathscr{F}(U_N)$ is Hermitian.

Implementation Details

- The Random Function U_N is periodic $\rightarrow$ restrict the evaluation to a domain.
- The Random Function U_N is complex. If a real approximation is desired, the sequence of partitions $(V_j^N)_{j\in\{1,\dots,N\},N\in\mathbb{N}_*}$ and the tag points $(\xi_j^N)_{j\in\{1,\dots,N\},N\in\mathbb{N}_*}$ must be selected such that $M_{U_N} = \mathscr{F}(U_N)$ is Hermitian.
- The Random Function U_N is smooth in mean-square. Regular models will be better approximated.

Implementation Details

- The Random Function U_N is periodic $\rightarrow$ restrict the evaluation to a domain.
- The Random Function U_N is complex. If a real approximation is desired, the sequence of partitions $(V_j^N)_{j\in\{1,\dots,N\},N\in\mathbb{N}_*}$ and the tag points $(\xi_j^N)_{j\in\{1,\dots,N\},N\in\mathbb{N}_*}$ must be selected such that $M_{U_N} = \mathscr{F}(U_N)$ is Hermitian.
- The Random Function U_N is smooth in mean-square. Regular models will be better approximated.
- The complex random variables $M_X(V_j^N)$ are non-correlated, but not necessarily independent. For instance, $M_X(V_j^N) = \overline{M_X}(-V_j^N)$.

Implementation Details

- The Random Function U_N is periodic $\rightarrow$ restrict the evaluation to a domain.
- The Random Function U_N is complex. If a real approximation is desired, the sequence of partitions $(V_j^N)_{j\in\{1,\dots,N\},N\in\mathbb{N}_*}$ and the tag points $(\xi_j^N)_{j\in\{1,\dots,N\},N\in\mathbb{N}_*}$ must be selected such that $M_{U_N} = \mathscr{F}(U_N)$ is Hermitian.
- The Random Function U_N is smooth in mean-square. Regular models will be better approximated.
- The complex random variables $M_X(V_j^N)$ are non-correlated, but not necessarily independent. For instance, $M_X(V_j^N) = \overline{M_X}(-V_j^N)$.
- The simulation of U_N can be computed for arbitrary tag points and over any arbitrary point x in the space. If the number of evaluation points is $M \in \mathbb{N}_*$, the algorithm has a complexity $\mathcal{O}(MN)$.

Implementation Details

- The Random Function U_N is periodic $\rightarrow$ restrict the evaluation to a domain.
- The Random Function U_N is complex. If a real approximation is desired, the sequence of partitions $(V_j^N)_{j\in\{1,...,N\},N\in\mathbb{N}_*}$ and the tag points $(\xi_j^N)_{j\in\{1,...,N\},N\in\mathbb{N}_*}$ must be selected such that $M_{U_N} = \mathscr{F}(U_N)$ is Hermitian.
- The Random Function U_N is smooth in mean-square. Regular models will be better approximated.
- The complex random variables $M_X(V_j^N)$ are non-correlated, but not necessarily independent. For instance, $M_X(V_j^N) = \overline{M_X}(-V_j^N)$.
- The simulation of U_N can be computed for arbitrary tag points and over any arbitrary point x in the space. If the number of evaluation points is $M \in \mathbb{N}_*$, the algorithm has a complexity $\mathcal{O}(MN)$.
- In order to apply fast computation algorithms as the FFT, we need both the tag points and the evaluation points to be set in convenient regular grids. In such a case the complexity is $\mathcal{O}(\log(M)N)$.

Implementation Details

Specifications

- All the spatial simulations are set over $[0, 100] \times [0, 100]$.
- The approximation order is $N = 2^{12}$ *in every axe*.
- The spatial regular grid, which depends on N, is of 567×567 points.

Matérn Model

$$(\kappa^2 - \Delta)^{\frac{\alpha}{2}} U = W \quad ; \quad g(\xi) = (\kappa^2 + |\xi|^2)^{\frac{\alpha}{2}} \tag{14}$$

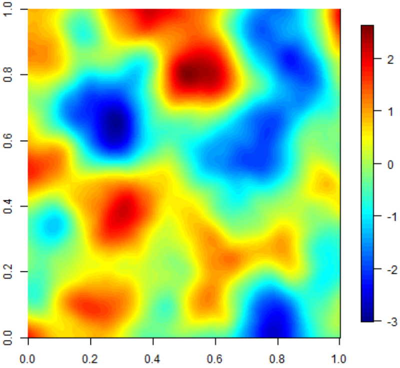

$\alpha = 4$, $\kappa = \frac{1}{5}$. Normalized variance.

Matérn Model

$$(\kappa^2 - \Delta)^{\frac{\alpha}{2}} U = W \quad ; \quad g(\xi) = (\kappa^2 + |\xi|^2)^{\frac{\alpha}{2}} \tag{15}$$

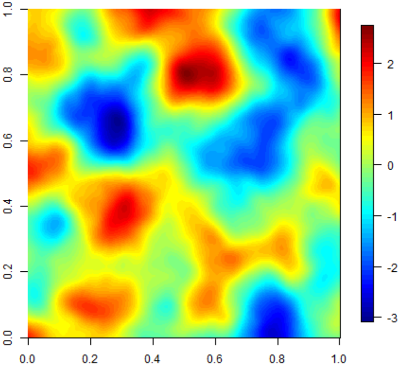

$\alpha = 3.67$, $\kappa = \frac{1}{5}$. Normalized variance.

Matérn Model

$$(\kappa^2 - \Delta)^{\frac{\alpha}{2}} U = W \quad ; \quad g(\xi) = (\kappa^2 + |\xi|^2)^{\frac{\alpha}{2}} \tag{16}$$

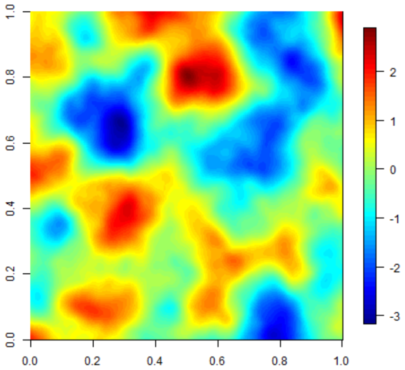

$\alpha = 3.33$, $\kappa = \frac{1}{5}$. Normalized variance.

Matérn Model

$$(\kappa^2 - \Delta)^{\frac{\alpha}{2}} U = W \quad ; \quad g(\xi) = (\kappa^2 + |\xi|^2)^{\frac{\alpha}{2}} \qquad (17)$$

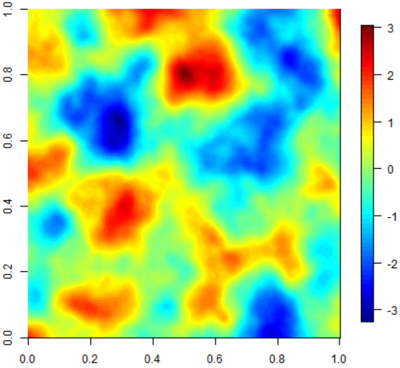

$\alpha = 3$, $\kappa = \frac{1}{5}$. Normalized variance.

Matérn Model

$$(\kappa^2 - \Delta)^{\frac{\alpha}{2}} U = W \quad ; \quad g(\xi) = (\kappa^2 + |\xi|^2)^{\frac{\alpha}{2}} \tag{18}$$

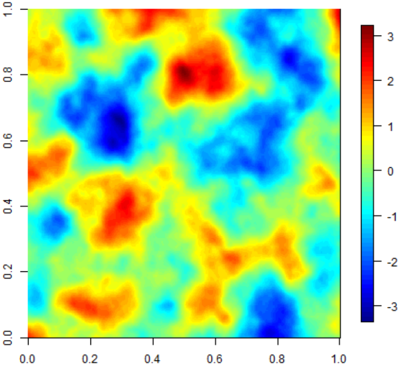

$\alpha = 2.67$, $\kappa = \frac{1}{5}$. Normalized variance.

$$(\kappa^2 - \Delta)^{\frac{\alpha}{2}} U = W \quad ; \quad g(\xi) = (\kappa^2 + |\xi|^2)^{\frac{\alpha}{2}} \tag{19}$$

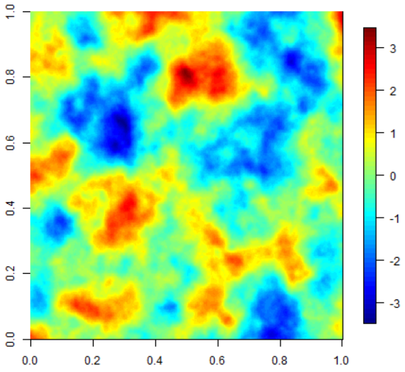

$\alpha = 2.33$, $\kappa = \frac{1}{5}$. Normalized variance.

Matérn Model

$$(\kappa^2 - \Delta)^{\frac{\alpha}{2}} U = W \quad ; \quad g(\xi) = (\kappa^2 + |\xi|^2)^{\frac{\alpha}{2}} \tag{20}$$

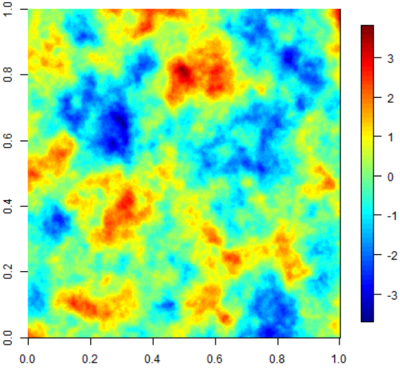

$\alpha = 2$, $\kappa = \frac{1}{5}$. Normalized variance.

Matérn Model

$$(\kappa^2 - \Delta)^{\frac{\alpha}{2}} U = W \quad ; \quad g(\xi) = (\kappa^2 + |\xi|^2)^{\frac{\alpha}{2}} \tag{21}$$

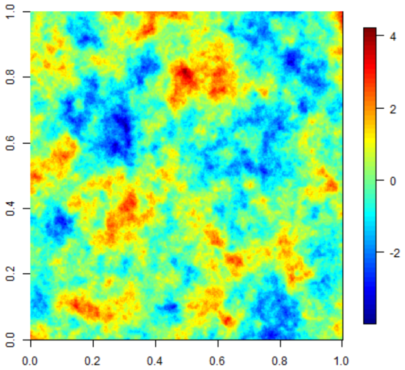

$\alpha = 1.67$, $\kappa = \frac{1}{5}$. Normalized variance.

Matérn Model

$$(\kappa^2 - \Delta)^{\frac{\alpha}{2}} U = W \quad ; \quad g(\xi) = (\kappa^2 + |\xi|^2)^{\frac{\alpha}{2}} \tag{22}$$

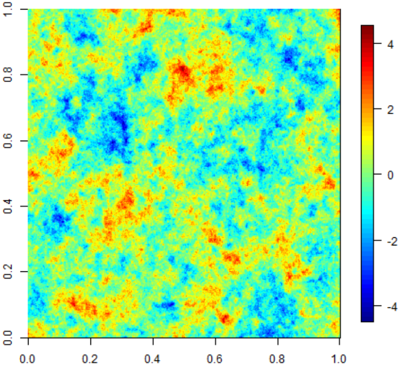

$\alpha = 1.33$, $\kappa = \frac{1}{5}$. Normalized variance.

Matérn Model

$$(\kappa^2 - \Delta)^{\frac{\alpha}{2}} U = W \quad ; \quad g(\xi) = (\kappa^2 + |\xi|^2)^{\frac{\alpha}{2}} \tag{23}$$

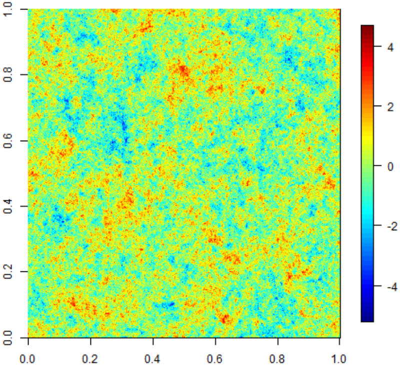

$\alpha = 1$, $\kappa = \frac{1}{5}$. Normalized variance.

Matérn Model

$$(\kappa^2 - \Delta)^{\frac{\alpha}{2}} U = W \quad ; \quad g(\xi) = (\kappa^2 + |\xi|^2)^{\frac{\alpha}{2}} \tag{24}$$

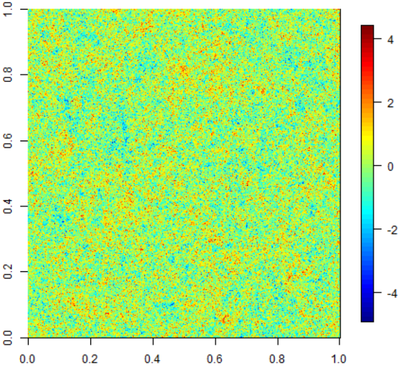

$\alpha = 0.67$, $\kappa = \frac{1}{5}$. Normalized variance.

Matérn Model

$$(\kappa^2 - \Delta)^{\frac{\alpha}{2}} U = W \quad ; \quad g(\xi) = (\kappa^2 + |\xi|^2)^{\frac{\alpha}{2}} \qquad (25)$$

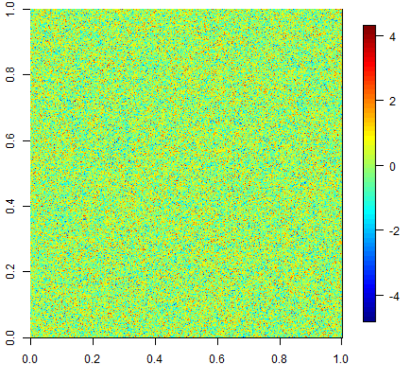

$\alpha = 0.33$, $\kappa = \frac{1}{5}$. Normalized variance.

Lim-Teo Generalization of Matérn model [Lim & Teo, 2009]

$$(\kappa^2 + (-\Delta)^\alpha)^{\frac{\gamma}{2}} U = W \quad ; \quad g(\xi) = (\kappa^2 + |\xi|^{2\alpha})^{\frac{\gamma}{2}} \tag{26}$$

Lim-Teo Generalization of Matérn model [Lim & Teo, 2009]

$$(\kappa^2 + (-\Delta)^\alpha)^{\frac{\gamma}{2}} U = W \quad ; \quad g(\xi) = (\kappa^2 + |\xi|^{2\alpha})^{\frac{\gamma}{2}} \tag{26}$$

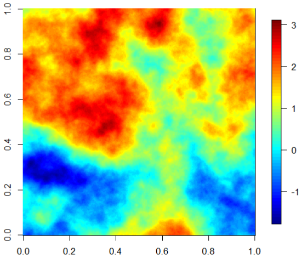

(a) $\alpha = 0.5$, $\gamma = 4$

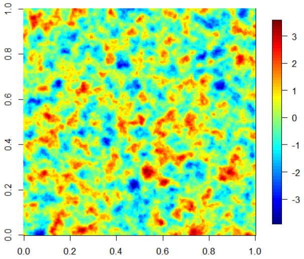

(b) $\alpha = 3$, $\gamma = \frac{2}{3}$

$\kappa = \frac{1}{5}$. Normalized variance.

Adding advections

$$\mathcal{L}_g U = W \quad ; \quad g(\xi) = g_R(\xi) + i g_I(\xi) \tag{27}$$

Example:

$$g(\xi) = g_R(\xi) + i v^T \xi \quad \rightarrow \quad \mathcal{L}_{g_R} U + v^T \nabla U = W, \tag{28}$$

for $v \in \mathbb{R}^d$.

Adding advections

$$\mathcal{L}_g U = W \quad ; \quad g(\xi) = g_R(\xi) + i g_I(\xi) \tag{27}$$

Example:

$$g(\xi) = g_R(\xi) + i v^T \xi \quad \rightarrow \quad \mathcal{L}_{g_R} U + v^T \nabla U = W, \tag{28}$$

for $v \in \mathbb{R}^d$.

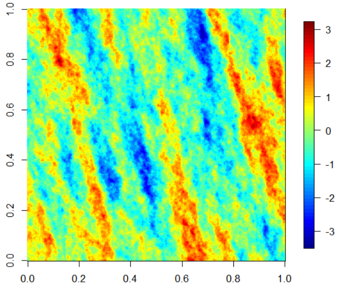

$g(\xi) = (\kappa^2 + |\xi|^2)^{\frac{\alpha}{2}} + i v^T \xi$. $\alpha = 2$, $\kappa = \frac{1}{5}$, $v = (-1, 4)$. Normalized variance.

Adding Advections

For less conventional advections:

$$g_I(\xi) = f(v^T \xi), \tag{29}$$

with f an odd function.

Adding Advections

For less conventional advections:

$$g_I(\xi) = f(v^T\xi), \tag{29}$$

with f an odd function.

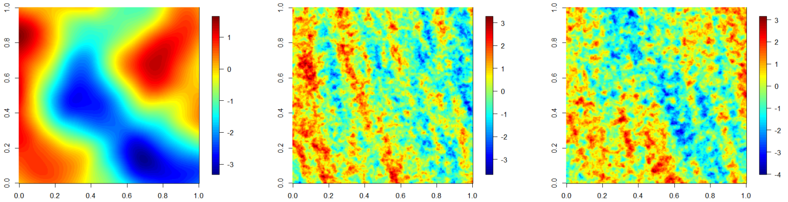

(a) $g(\xi) = (\kappa^2 + |\xi|^2)^{\frac{\alpha}{2}} + i(v^T\xi)^3$ (b) $g(\xi) = (\kappa^2 + |\xi|^2)^{\frac{\alpha}{2}} + i\arctan(v^T\xi)$ (c) $g(\xi) = (\kappa^2 + |\xi|^2)^{\frac{\alpha}{2}} + i\sin(v^T\xi)$

$\kappa = \frac{1}{5}$, $\alpha = 2$, $v = (-1, 4)$. Normalized variance.

Separated Regularity

$$\left(\kappa^2 + \left(-\frac{\partial^2}{\partial x_1^2}\right)^{\alpha_1} + \left(-\frac{\partial^2}{\partial x_2^2}\right)^{\alpha_2}\right) U = W \quad ; \quad g(\xi) = \kappa^2 + |\xi_1|^{2\alpha_1} + |\xi_2|^{2\alpha_2} \tag{30}$$

Separated Regularity

$$\left(\kappa^2 + \left(-\frac{\partial^2}{\partial x_1^2}\right)^{\alpha_1} + \left(-\frac{\partial^2}{\partial x_2^2}\right)^{\alpha_2}\right) U = W \quad ; \quad g(\xi) = \kappa^2 + |\xi_1|^{2\alpha_1} + |\xi_2|^{2\alpha_2} \tag{30}$$

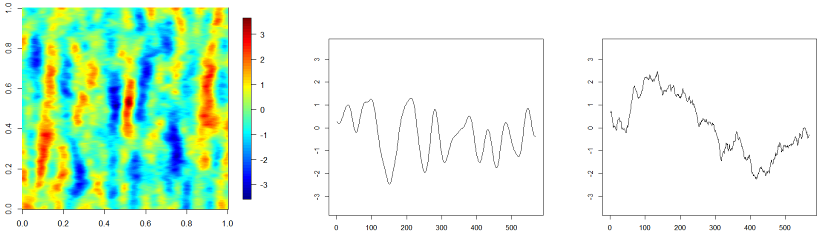

(a) $\alpha_1 = 3$, $\alpha_2 = 0.7$ (b) Trace at a fixed x_2 (c) Trace at a fixed x_1

$\kappa^2 = \left(\frac{1}{5}\right)^2$. Normalized variance.

Separated Regularity + Asymmetries

$$\left(\kappa^2 - \frac{\partial^2}{\partial x_1^2}\right)^{\frac{\alpha}{2}} U + \frac{\partial^\beta U}{\partial x_2^\beta} = W \quad ; \quad g(\xi) = (\kappa^2 + |\xi_1|^2)^{\frac{\alpha}{2}} + (i\xi_2)^\beta \tag{31}$$

Separated Regularity + Asymmetries

$$\left(\kappa^2 - \frac{\partial^2}{\partial x_1^2}\right)^{\frac{\alpha}{2}} U + \frac{\partial^\beta U}{\partial x_2^\beta} = W \quad ; \quad g(\xi) = (\kappa^2 + |\xi_1|^2)^{\frac{\alpha}{2}} + (i\xi_2)^\beta \qquad (31)$$

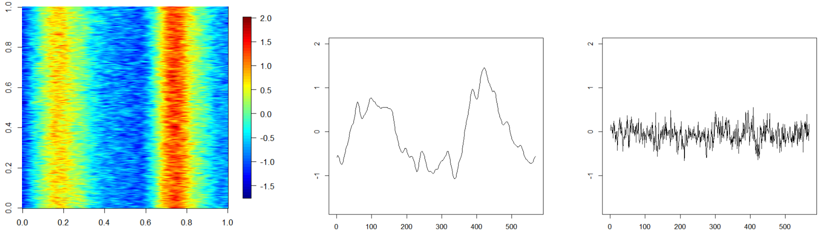

(a) $\alpha = 4$, $\beta = 0.7$ (b) Trace at a fixed x_2 (c) Trace at a fixed x_1

$\kappa^2 = \left(\frac{1}{5}\right)^2$. Normalized variance.

Separated Regularity + Asymmetries

$$\left(\kappa^2 - \frac{\partial^2}{\partial x_1^2}\right)^{\frac{\alpha}{2}} U + \frac{\partial^\beta U}{\partial x_2^\beta} = W \quad ; \quad g(\xi) = (\kappa^2 + |\xi_1|^2)^{\frac{\alpha}{2}} + (i\xi_2)^\beta \tag{32}$$

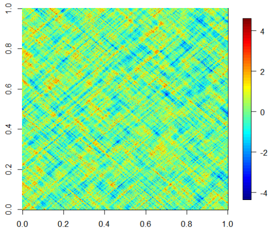

(a) $\alpha = 2$, $\beta = 1.8$

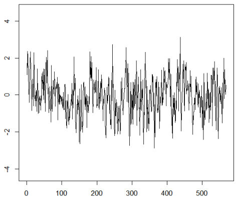

(b) Trace at a fixed x_2

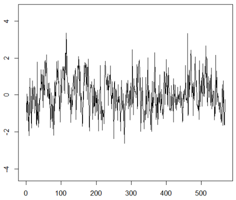

(c) Trace at a fixed x_1

$\kappa^2 = \left(\frac{1}{5}\right)^2$. Normalized variance.

$$\left(\kappa^2 - \frac{\partial^2}{\partial x_1^2}\right)^{\frac{\alpha}{2}} U + \frac{\partial^\beta U}{\partial x_2^\beta} = W \quad ; \quad g(\xi) = (\kappa^2 + |\xi_1|^2)^{\frac{\alpha}{2}} + (i\xi_2)^\beta \qquad (33)$$

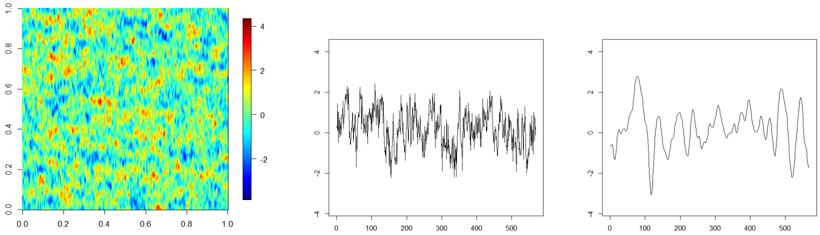

(a) $\alpha = 0.7$, $\beta = 4$ (b) Trace at a fixed x_2 (c) Trace at a fixed x_1

$\kappa^2 = \left(\frac{1}{5}\right)^2$. Normalized variance.

Section 4

Some Spatio-temporal SPDE-based models

Implementation details

Specifications

- We keep the same spatial domain $[0, 100] \times [0, 100]$.
- We simulate over regular temporal grids of step $dt = 0.1$, considering 100 time steps.
- The approximations are *spatial*. The models presented satisfy *exactly* the spatio-temporal SPDE presented.

First Order Evolution Model

$$\begin{cases} \dfrac{\partial U}{\partial t} + \mathcal{L}_g U = X_S \otimes W_T \\ U\Big|_{t=0} = U_0 \end{cases} . \tag{34}$$

First Order Evolution Model

$$\begin{cases} \dfrac{\partial U}{\partial t} + \mathcal{L}_g U = X_S \otimes W_T \\ U\Big|_{t=0} = U_0 \end{cases} . \tag{34}$$

- U_0: a stationary spatial initial condition.

First Order Evolution Model

$$\begin{cases} \frac{\partial U}{\partial t} + \mathcal{L}_g U = X_S \otimes W_T \\ U\Big|_{t=0} = U_0 \end{cases} . \quad (34)$$

- U_0: a stationary spatial initial condition.
- $X_S \otimes W_T$: coloured in space, white-in-time noise, independent of U_0 (X_S represents any spatial stationary random field).

First Order Evolution Model

$$\begin{cases} \dfrac{\partial U}{\partial t} + \mathcal{L}_g U = X_S \otimes W_T \\ U\Big|_{t=0} = U_0 \end{cases} . \tag{34}$$

- U_0: a stationary spatial initial condition.
- $X_S \otimes W_T$: coloured in space, white-in-time noise, independent of U_0 (X_S represents any spatial stationary random field).
- $g : \mathbb{R}^d \to \mathbb{C}$ a *spatial* symbol function, with $\Re g \geq \kappa$ for some $\kappa > 0$.

First Order Evolution Model

$$\begin{cases} \dfrac{\partial U}{\partial t} + \mathcal{L}_g U = X_S \otimes W_T \\ U\Big|_{t=0} = U_0 \end{cases} . \quad (34)$$

- U_0: a stationary spatial initial condition.
- $X_S \otimes W_T$: coloured in space, white-in-time noise, independent of U_0 (X_S represents any spatial stationary random field).
- $g : \mathbb{R}^d \to \mathbb{C}$ a *spatial* symbol function, with $\Re g \geq \kappa$ for some $\kappa > 0$.
- $\mathcal{L}_g = \mathscr{F}_S^{-1}(g \mathscr{F}_S(\cdot))$.

Following [Sigrist et al., 2015]

We use our approximation method *spatially*, and solve *explicitly* the equation in time.

First Order Evolution Model

$$\begin{cases} \dfrac{\partial U}{\partial t} + v^T \nabla U + (\kappa^2 - \Delta)^{\frac{\alpha}{2}} U = X_S \otimes W_T \\ U\big|_{t=0} = 0 \end{cases} . \quad (35)$$

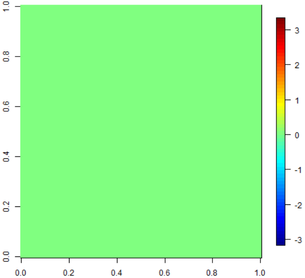

$\kappa = \left(\frac{1}{5}\right)^2$, $\alpha = 3.12$, $v = (2,5)$. X_S Matérn with $\kappa_{X_S}^2 = \left(\frac{1}{5}\right)^2$, $\alpha_{X_S} = 0.65$.

First Order Evolution Model

$$\begin{cases} \dfrac{\partial U}{\partial t} + v^T \nabla U + (\kappa^2 + (-\Delta)^{\alpha})^{\frac{\gamma}{2}} U = X_S \otimes W_T \\ U\big|_{t=0} = W_0 \end{cases} \quad . \qquad (36)$$

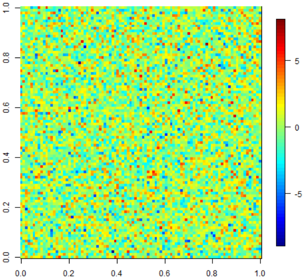

$\kappa = \left(\frac{1}{5}\right)^2$, $\alpha = 3.12$, $\gamma = 0.75$, $v = (-2, -5)$. X_S with separated regularities, $\kappa^2_{X_S} = \left(\frac{1}{5}\right)^2$, $\alpha_{X_S,1} = 2.3$. $\alpha_{X_S,1} = 0.7$. W_0 a unitary spatial White Noise.

Waving Models

Stationary solutions for the Homogeneous Wave Equation:

$$\frac{\partial^2 U}{\partial t^2} - c^2 \Delta U = 0. \tag{37}$$

Waving Models

Stationary solutions for the Homogeneous Wave Equation:

$$\frac{\partial^2 U}{\partial t^2} - c^2 \Delta U = 0. \tag{37}$$

It can be shown [Carrizo Vergara et al., 2018] that there are infinitely many possible stationary models following this equation, for which we can *control its spatial behaviour arbitrarily*.

Waving Models

Stationary solutions for the Homogeneous Wave Equation:

$$\frac{\partial^2 U}{\partial t^2} - c^2 \Delta U = 0. \tag{37}$$

It can be shown [Carrizo Vergara et al., 2018] that there are infinitely many possible stationary models following this equation, for which we can *control its spatial behaviour arbitrarily*.

Adaptation

We select the tag-points in $\mathbb{R}^d \times \mathbb{R}$ being set over the *spatio-temporal cone:*

$$\{(\xi, \omega) \in \mathbb{R}^d \times \mathbb{R} \;\big|\; |\omega| = c|\xi|\}, \tag{38}$$

which is the set where the spatio-temporal symbol function $g(\xi, \omega) = -\omega^2 + c^2|\xi|^2$ is null. Then, we apply a spatio-temporal Fourier Transform.

$$\begin{cases} \frac{\partial^2 U}{\partial t^2} - c^2 \Delta U = 0 & \text{over } \mathbb{R}^d \times \mathbb{R} \\ a(\kappa^2 - \Delta)^{\frac{\alpha}{2}} U_S \overset{2nd\ o}{=} W_S & \text{over } \mathbb{R}^d \end{cases} . \quad (39)$$

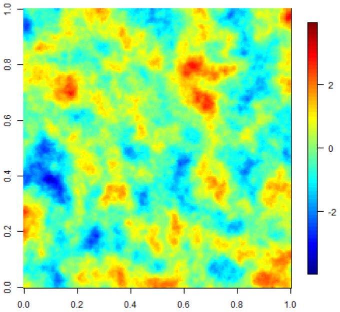

$\kappa^2 = \left(\frac{1}{5}\right)^2$, $\alpha = 2$, $c = 8$. a is a normalizing constant.

Waving Models

$$
\begin{cases} \frac{\partial^2 U}{\partial t^2} - c^2 \Delta U = 0 & \text{over } \mathbb{R}^d \times \mathbb{R} \\ a(\kappa^2 - \Delta)^{\frac{\alpha}{2}} U_S \overset{2nd\ o}{=} W_S & \text{over } \mathbb{R}^d \end{cases} . \quad (40)
$$

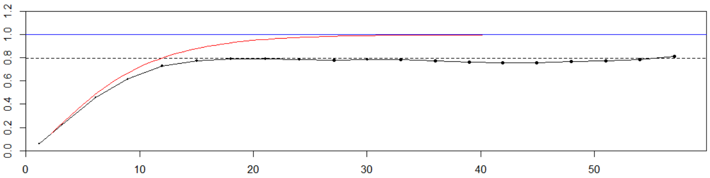

Spatial experimental variograms. In red, the theoretical Matérn variogram with unitary variance remarked in blue.

Section 5

Discussion

Discussion

Advantages

- HUGE freedom and generality. Able to study models related to a wide-class of SPDEs having interesting properties.

Discussion

Advantages

- HUGE freedom and generality. Able to study models related to a wide-class of SPDEs having interesting properties.
- Easy adaptability to spatio-temporal context with non-trivial properties and presenting traditional physical meaning.

Discussion

Advantages

- HUGE freedom and generality. Able to study models related to a wide-class of SPDEs having interesting properties.
- Easy adaptability to spatio-temporal context with non-trivial properties and presenting traditional physical meaning.
- Fast computation when using the FFT algorithm.

Discussion

Advantages

- HUGE freedom and generality. Able to study models related to a wide-class of SPDEs having interesting properties.
- Easy adaptability to spatio-temporal context with non-trivial properties and presenting traditional physical meaning.
- Fast computation when using the FFT algorithm.

Disadvantages

- Memory consuming.

Discussion

Advantages

- HUGE freedom and generality. Able to study models related to a wide-class of SPDEs having interesting properties.
- Easy adaptability to spatio-temporal context with non-trivial properties and presenting traditional physical meaning.
- Fast computation when using the FFT algorithm.

Disadvantages

- Memory consuming.
- Not immediate expression for precision matrices for irregular data. Not sparsity. The method is not immediately adapted to make inferences as the FEM does.

Discussion

Advantages

- HUGE freedom and generality. Able to study models related to a wide-class of SPDEs having interesting properties.
- Easy adaptability to spatio-temporal context with non-trivial properties and presenting traditional physical meaning.
- Fast computation when using the FFT algorithm.

Disadvantages

- Memory consuming.
- Not immediate expression for precision matrices for irregular data. Not sparsity. The method is not immediately adapted to make inferences as the FEM does.
- The convergence of the approximation to the target model are slower than expected, requiring higher computational costs to have good approximations specially in cases with low regularity.

Matérn Model: Qualitative Error Analysis

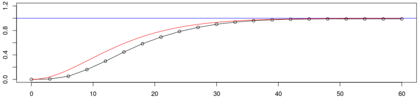

(a) $N = 2^{10}$

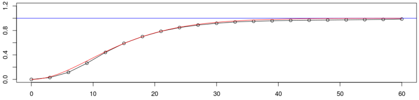

(b) $N = 2^{11}$

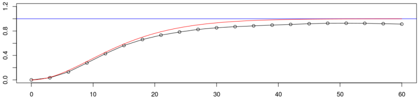

(c) $N = 2^{12}$

$\alpha = 4$, $\kappa^2 = \left(\frac{1}{5}\right)^2$. Comparison between the avarage of the experimental variogram of 50 independent simulations and the target Matérn variogram. Normalized.

Matérn Model: Qualitative Error Analysis

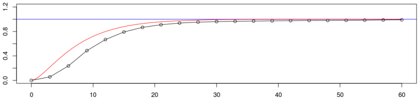

(a) $N = 2^{10}$

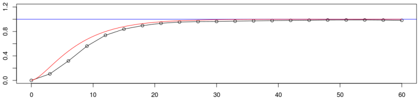

(b) $N = 2^{11}$

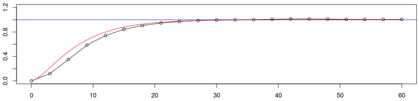

(c) $N = 2^{12}$

$\alpha = 2$, $\kappa^2 = \left(\frac{1}{5}\right)^2$. Comparison between the avarage of the experimental variogram of 50 independent simulations and the target Matérn variogram. Normalized.

Matérn Model: Qualitative Error Analysis

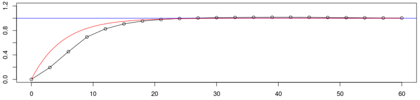

(a) $N = 2^{10}$

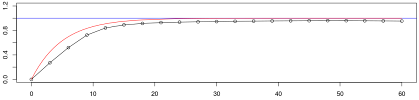

(b) $N = 2^{11}$

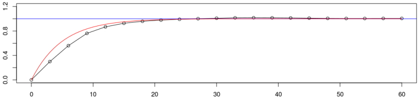

(c) $N = 2^{12}$

$\alpha = 1.5$, $\kappa^2 = \left(\frac{1}{5}\right)^2$. Comparison between the avarage of the experimental variogram of 50 independent simulations and the target Matérn variogram. Normalized.

Section 6

MUCHAS GRACIAS

References

Carrizo Vergara, R., Desassis, N. , Allard, D. (2018). A general framework for SPDE-based stationary random fields. *arXiv preprint arXiv:1806.04999.*

Lang, A. and Potthoff, J. (2011). Fast simulation of Gaussian random fields. *Monte Carlo Methods and Applications, 17(3)*, 195-214.

Lim, S.C. and Teo, L.P. (2009). Generalized Whittle-Matérn random field as a model of correlated fluctuations. *Journal of Physics A: Mathematical and Theoretical, 42(10)*.

Lindgren F., Rue H. and Lindström J. (2011). An explicit link between Gaussian fields and Gaussian Markov random fields: the stochastic partial differential equation approach. *Journal of the Royal Statistical Society: Series B, 73(4)*, 423-498.

Pardo-Iguzquiza, E. and Chica-Olmo, M. (1993). The Fourier integral method: an efficient spectral method for simulation of random fields. *Mathematical Geology, 25(2)*, 177-217.

Sigrist, F., Künsch, H. R., and Stahel, W. A. (2015). Stochastic partial differential equation based modeling of large space-time data sets. *Journal of the Royal Statistical Society: Series B (Statistical Methodology), 77*(1), 3-33.